Synergistic dispersal of plant pathogen spores by jumping-droplet condensation and wind

Ranit Mukherjee[a] , Hope A. Gruszewski[b], Landon T. Bilyeu[b], David G. Schmale III[b], and Jonathan B. Boreyko[c,1]

[a]Department of Biomedical Engineering and Mechanics, Virginia Tech, Blacksburg, VA 24061; [b]School of Plant and Environmental Sciences, Virginia Tech, Blacksburg, VA 24061; and [c]Department of Mechanical Engineering, Virginia Tech, Blacksburg, VA 24061

Plant pathogens are responsible for the annual yield loss of crops worldwide and pose a significant threat to global food security. A necessary prelude to many plant disease epidemics is the short-range dispersal of spores, which may generate several disease foci within a field. New information is needed on the mechanisms of plant pathogen spread within and among susceptible plants. Here, we show that self-propelled jumping dew droplets, working synergistically with low wind flow, can propel spores of a fungal plant pathogen (wheat leaf rust) beyond the quiescent boundary layer and disperse them onto neighboring leaves downwind. An array of horizontal water-sensitive papers was used to mimic healthy wheat leaves and showed that up to 25 spores/h may be deposited on a single leaf downwind of the infected leaf during a single dew cycle. These findings reveal that a single dew cycle can disperse copious numbers of fungal spores to other wheat plants, even in the absence of rain splash or strong gusts of wind.

wheat leaf rust | jumping-droplet condensation | pathogen transport | wind dispersal | fungicide

Spores of plant pathogenic fungi are spread through the atmosphere in three stages: liberation from the host by some active or passive method(s), drift by biotic or abiotic factors, and deposition onto a new host (1). Examples of active liberation mechanisms include osmotic pressure–driven ejection of ascospores of *Fusarium graminearum* (the causal agent of Fusarium head blight of wheat) and ballistospore ejection from the tip of a sterigma due to the chemical secretion of a Buller's drop (2, 3). In the absence of wind, the resulting dispersal distance is a function of both the weight of the spore(s) and the initial discharge velocity, with the range of discharge varying from 40 μm for basidiospores (4) to 6 m for the artillery fungus (5). Passive liberation and dispersal mechanisms, such as wind and rain splash, can spread fungal diseases in plants (6). For wind to successfully liberate dry spores, an unusually strong and/or sudden gust of wind is often required (1, 6–9). In contrast, rain splash can liberate spores from a plant either through transferring momentum to the leaf to launch spores off (10, 11) or by adhering spores to splashed satellite droplets (12, 13). Spores ejected by active methods or rain splash can only disperse over a very short distance in the absence of wind (14) but when carried in moderate winds, can travel for many kilometers (15, 16).

One recent study reported an entirely new mode of pathogen liberation, where coalescing dew droplets on superhydrophobic wheat leaves jump with considerable velocity (0.1 to 1.0 m/s) and carry adhered spores of a fungal plant pathogen (17). Mechanistically, the out-of-plane motion is a result of symmetry breaking as the expanding liquid bridge during coalescence impinges upon the bottom substrate (18–20) (Fig. 1A). While this initial report characterized the jumping-droplet liberation of spores in the absence of wind (17), it did not consider the subsequent dispersal or deposition, which ultimately governs the rate of disease spread. Here, we characterize the dispersal of spores of leaf rust (*Puccinia triticina*) after they are liberated from a diseased wheat

leaf via jumping-droplet condensation. Two different scenarios are explored: short-range and long-range drift and deposition in the absence and presence of wind flow, respectively (Fig. 1 B and C). We found that even a low wind speed (0.5 m/s) is capable of dispersing as many as 100 jumping droplets and 25 spores to a single leaf downwind of a diseased leaf saturated in dew. Our ability to quantify both the liberation and dispersal of fungal spores from a diseased leaf during a dew cycle improves our understanding of disease spread within and among plants (1, 21–23).

Results

Range of Spore Dispersal via Jumping-Droplet Condensation Alone. To explore the short-range dispersal of rust spores without any wind flow, we bonded a piece of a wheat leaf (*SI Appendix,* Fig. S1) to a horizontal cold plate with thermal paste (Fig. 2A) and decreased the plate temperature below the dew point temperature. Due to the nanoscale surface asperities on the wheat leaves, which render them superhydrophobic (*SI Appendix,* Fig. S2 A and B and section 2), jumping-droplet condensation was observed on the diseased wheat leaves where coalescing droplets jumped off the surface with or without spore(s) (17). After a sufficient (i.e., steady-state surface coverage) amount of condensates formed on the leaf (*SI Appendix,* Fig. S3) (which took about 15 to 30 min depending on the laboratory air temperature and humidity), a water-sensitive paper was placed on a lower platform about 1 cm below the leaf on the upper cold

Significance

Some fungal diseases spread within and among crops via the aerial dispersal of microscopic spores. Existing studies have characterized the liberation and dispersal of spores via wind and/or rain splash. Here, we show that dew droplets spontaneously jumping from superhydrophobic wheat leaves can disperse adhered spores, even in the complete absence of rain or strong winds. We found that the jumping-droplet effect results in short-range spore dispersal in the absence of wind. Long-range dispersal was possible when jumped droplets became suspended in a gentle wind, which is a synergistic effect as the wind alone was unable to dislodge dry spores. Finally, we show that proactive measures, such as applying a fungicide to suppress jumping-droplet condensation, can prevent dew-induced disease spread.

Fig. 1. Spore dispersal via jumping-droplet condensation. (*A*) Jumping-droplet condensation on a healthy wheat leaf. Two condensed droplets coalesce (second frame) and jump off from the superhydrophobic wheat leaf (third frame). (*B*) Without any wind, the jumped droplets with spores can land on an adjacent healthy leaf, spreading the disease within the plant. (*C*) In low (0.5 m/s) to moderate (1.5 m/s) wind speed, the spore-laden jumped droplets can travel long-range to land on different healthy plants within the field.

plate. After each trial, the water-sensitive paper was analyzed under a top-down optical microscope (*SI Appendix*, Fig. S4*A*). Impacted water droplets created quasicircular dark blue stains on the paper, while adhered spores were directly visible as brown quasispherical objects (*SI Appendix*, Fig. S5). Three different measurements were made from the water-sensitive paper: the number of spores within each droplet stain, the final lateral distance (i.e., stain location) of a jumping droplet from the edge of the overlying leaf (l_f), and the maximum diameter of the stains (D_{max}).

With this information, a dispersal gradient was generated, which showed the spatial variation in the spore number density with increasing distance from the source (24). A modification to the classical dispersal gradient was necessary for our jumping-droplet spore dispersal, as the number of spores within each jumped droplet varied significantly. Therefore, we made a three-dimensional frequency plot (Fig. 2*B*), which quantified both the number of droplets and the number of spores per droplet at any given distance from the source leaf. It is evident from the plot that the majority of the
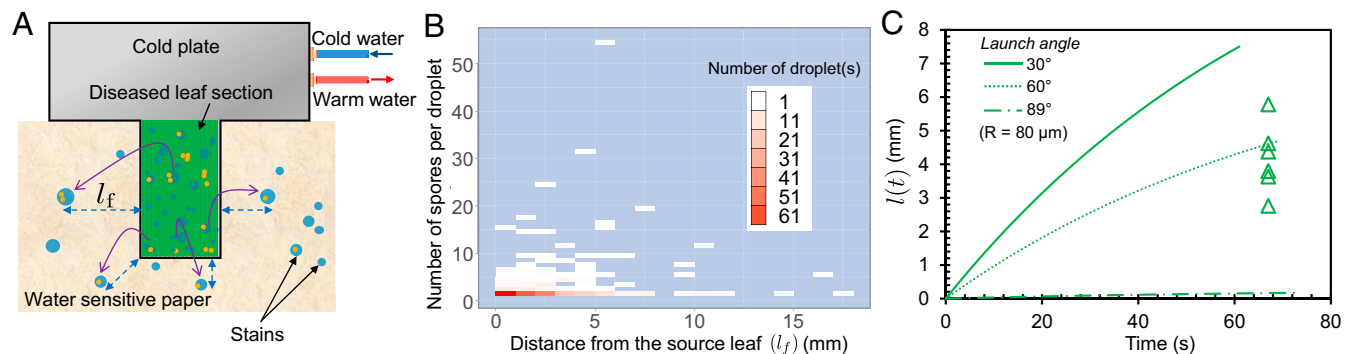
Fig. 2. Spore dispersal in the no-wind condition. (*A*) Experimental laboratory setup to find the range of dispersal of jumping-droplet condensates with spores in the no-wind condition. The water-sensitive paper was analyzed under a microscope, and the distance l_f from the edge of the leaf was measured for each droplet stain containing a spore(s). (*B*) Frequency plot showing the number of spore-laden droplets vs. the lateral impact distance from the source leaf. The *y* axis shows the number of spores in each droplet. (*C*) Theoretical range for an 80-μm droplet with three different jumping angles: $\theta_j = 30°$ (solid curve), $60°$ (dotted curve), and $89°$ (dotted-dashed curve). Experimentally obtained l_f values (green triangles) are superimposed for droplets whose splash diameter corresponded to a preimpact radius of $R = 84 \pm 5$ μm, as determined from the spread factors.

spore-carrying droplets ($\approx$57%, 193/340) jumping from the diseased leaf contained only one spore. About 39% (134/340) of the spore-carrying droplets contained 2 to 10 spores, and in rare cases ($\approx$4%, 13/340), droplets contained more than 10 spores. In one case, a droplet contained 55 spores. In terms of the lateral jumping distance from the edge of the leaf, the spore-laden droplet counts were highest within $l_f = 7.5$ mm ($\approx$95%, 323/340). The location of the remaining spore-laden droplets ranged from $l_f = 7.5$ to 17.5 mm. Thus, even without any appreciable wind, spores can disperse to other leaves of the same plant or leaves of a neighboring plant for a dense canopy (25) powered entirely by jumping-droplet condensation.

To rationalize the experimental measurements of l_f, the theoretical range of a jumped droplet was calculated. Specifically, we solved the equation of motion for a spherical projectile (i.e., a spore-laden droplet) of radius R, launched with an initial velocity u at angle θ_j with respect to the horizontal leaf surface. The jumping velocity is capillary-inertial: $u \approx 0.22(\gamma/\rho R)^{1/2}$, where γ and ρ are the surface tension and the density of water, respectively, and the 0.22 prefactor accounts for the surface energy that is lost to oscillatory (rather than translational) kinetic energy (18–20). It was not possible to correlate a stain on the water-sensitive paper with the angle (θ_j) of the corresponding coalesced droplet jumping from the leaf. However, previous studies of jumping-droplet condensation have reported that wide ranges of jumping angles are possible: $\theta_j = 10°$ to $90°$, with the value depending on the number, size, and geometric arrangement of the droplets coalescing together as well as the underlying surface microstructures (17, 26–28).

The preimpact radius (R) of a droplet can be estimated from the stain diameter ($D_{\max}$) using the spread factor, which is the ratio of stain diameter over the impacting droplet diameter. Spread factor values corresponding to the strain diameters on the water-sensitive papers were extracted from the plots provided with the product data sheet (*SI Appendix*, Fig. S6 and section 3). Here, we have assumed that all the jumped droplets have impacted the paper with terminal or sedimentation velocity, $V = 2\rho g R^2/9\mu_a$, where ρ and μ_a are the water density and air dynamic viscosity, respectively (29). For $D_{\max}$, we only considered nonoverlapping stains with at least one spore. Using the spread factor relation, the droplet radius range was found to be $R = 11$ to 147 μm.

Using the equation of motion for the specific case of $R = 80$ μm (*SI Appendix*, Fig. S7 and section 4 have the derivation), Fig. 2C graphs the lateral displacement (l) of a jumping droplet as a function of time. The three different displacement curves correspond to three different representative jumping angles: $\theta_j = 30°, 60°, 89°$. Each curve stops at a critical time of flight (t_c) where the droplet is predicted to impact the water-sensitive paper, such that $l(t_c) = l_f$. The minimum theoretical value of l_f was 0.17 mm for $\theta_j = 89°$, and the maximum value was 7.46 mm for $\theta_j = 30°$. Additionally, the experimentally measured values of l_f were plotted (green triangles) also for the case study of $R = 84 \pm 5$ μm as obtained from the spread factor and stain diameter relation. For the time axis, all the experimental plot points were placed at the average time-of-flight value for the three launch angles. The experimental values for l_f all fall within the boundaries set by the theoretical equation of motion. Similar plots for other droplet sizes ($R = 60, 100$ μm) are included in *SI Appendix*, Fig. S8. For these other cases, some droplets exhibited an l_f that exceeded the theoretical boundaries, which high-speed imaging confirmed was due to the droplets getting boosted during their descent by the laboratory's air circulation (Movie S1).
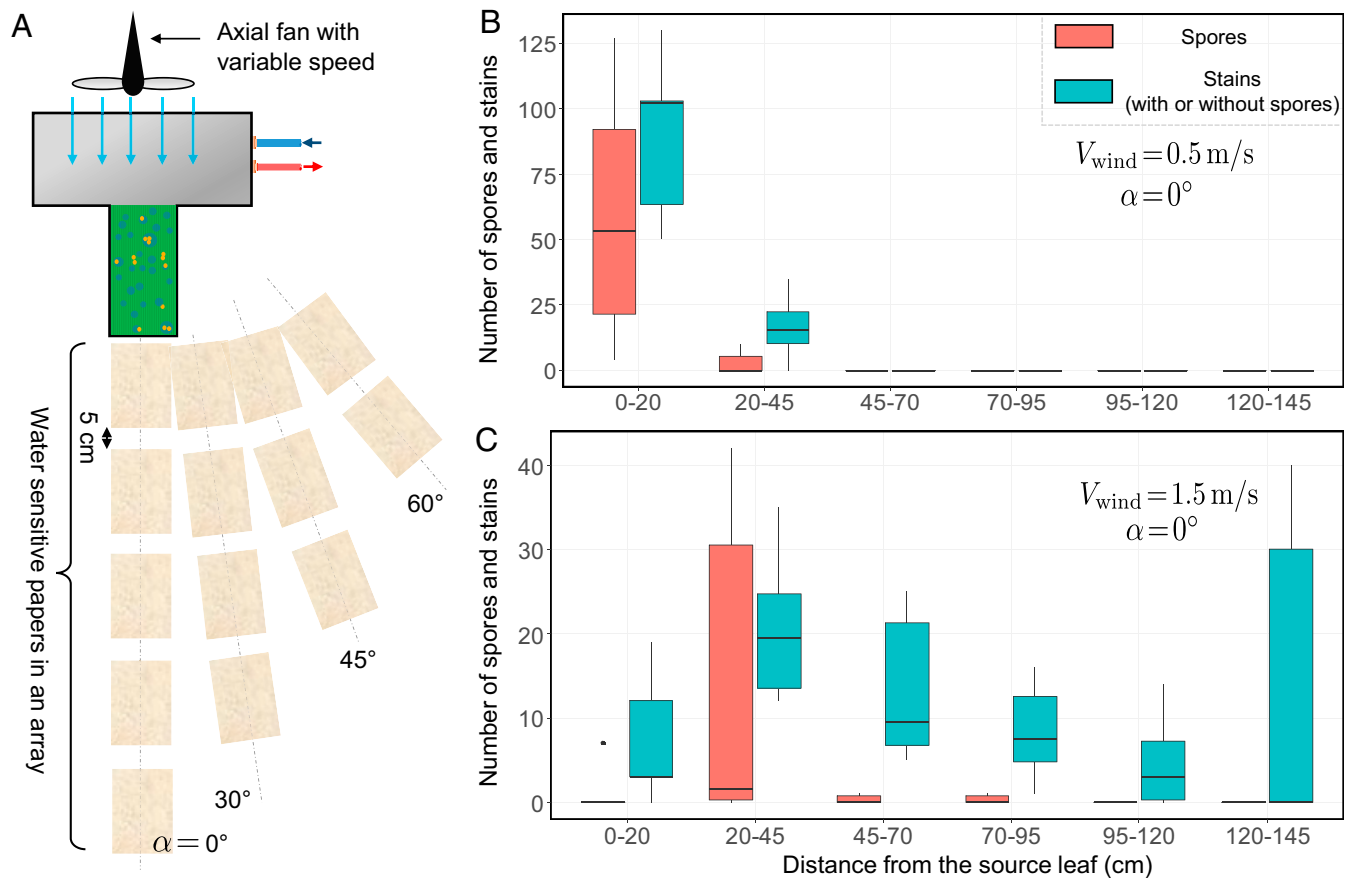
Range of Spore Dispersal via Jumping-Droplet Condensation in the Presence of Wind.

We showed that jumping-droplet condensation alone can liberate spores from a diseased leaf, enabling the possibility of multiple disease foci within a plant or neighboring plants (provided optimal environmental conditions and susceptible hosts). However, it is evidently not effective in dispersing the spores beyond a few millimeters. As with other passive methods of spore liberation, we should now consider how wind can enhance the range of the subsequent dispersal. In our case, the wind becomes especially relevant after a spore-laden jumping droplet clears the thin laminar boundary layer above the leaf. Thus, it is important to consider the synergistic effect of condensation and wind in spore dissemination, similar to how wind affects spore dispersal by rain splash (30). Simulating the effect of wind in a laboratory setting is challenging for several reasons. First, the wind increases the spatiotemporal scale of the spore transport (14). Second, higher wind speeds can be detrimental for the growth of condensate droplets on the leaf, diminishing the jumping-droplet effect. Third, a wind speed higher than a critical value can shear off the droplets from the leaf surface before they can jump via coalescence. In this report, we have used two separate wind speeds for the experiments, 0.5 and 1.5 m/s, comparable with the maximum favorable wind speed for dew formation on radiantly cooled surfaces (31), but much lower than the critical wind speed of about 10 m/s for shearing off the spore-laden micrometric droplets off the leaf surface (17).

A previous report by Nath et al. (17) showed that spore-laden condensate from a diseased wheat leaf can jump a vertical distance that tends to range from 1 to 5 mm. We needed to determine whether this jumping distance is enough to clear the quiescent boundary layer above the leaf's surface. The laminar boundary-layer thickness δ above a horizontal leaf surface for a free stream wind velocity U can be estimated as $\delta \sim \left(\frac{\nu x}{U}\right)^{1/2}$ (17), where $x \approx 3$ cm is the leaf length along the wind flow direction and $\nu = 1.5 \times 10^{-5}$ m²s⁻¹ is the air kinematic viscosity. With this, $\delta \approx 0.95$ mm for $U = 0.5$ m/s, and $\delta \approx 0.55$ mm for $U = 1.5$ m/s, both less than the characteristic jumping height. The top face of the wheat leaf contains micrometric bumps (*SI Appendix*, Fig. S2B), which are larger than some of the coalescing condensates (*SI Appendix*, Fig. S3). While most droplets did jump at angles approaching $90°$, droplets coalescing near the side walls of the bumps can jump sideways (17, 26–28), resulting in a subset of jumps with much lower jumping angles (*SI Appendix*, Fig. S9). For droplets jumping at angles much less than $90°$, obviously the chances of escaping the boundary layer decrease (although the odds of clearing the leaf edge increase). Regardless, our hypothesis is that in the majority of the jumping events, droplets will cross the slow-moving boundary layer to be carried away by the overlying free stream. We tested this hypothesis in the following experiments involving wind-induced dispersal.

The experimental setup involved a variable-speed axial fan placed about 10 cm behind the leaf (Fig. 3A and *SI Appendix*, Fig. S10). Water-sensitive papers were arranged in linear arrays with an edge-to-edge distance of 5 cm between each paper. One array of papers was placed directly along the axis of the wind flow ($\alpha = 0°$), up to a maximum distance of 1.5 m in front of the leaf. Three additional linear arrays of papers were placed at $\alpha = 30°, 45°$, and $60°$ with respect to the wind flow. After enough condensate droplets were grown on the leaf, the experiment commenced by turning the fan on. The desired wind speed above the leaf was achieved by adjusting the fan speed and/or by changing the distance between the leaf and the fan. The wind speed was measured with an anemometer placed about 1 cm above the leaf, an order of magnitude higher than the boundary-layer thickness. The water-sensitive papers with the blue stains were collected after 1 h of the fan being on and analyzed under the microscope. As most of the stains (with and without spores) were found on the papers along the $\alpha = 0°$ line, only those results are plotted here. *SI Appendix*, Figs. S11 and S12 have the results from the angled arrays.

Mukherjee et al.
Synergistic dispersal of plant pathogen spores by jumping-droplet condensation and wind

PNAS | 3 of 8
https://doi.org/10.1073/pnas.2106938118

Fig. 3. Spore dispersal in low to moderate wind conditions. (*A*) A variable-speed axial fan was introduced in the setup to achieve low to moderate wind conditions over the leaf surface. The water-sensitive papers were placed in an array downwind of the leaf with a gap of 5 cm between each paper. To cover a large area around the source, the paper arrays were placed in four different angles. (*B* and *C*) The number of stains (with or without spores) and the number of spores per paper are plotted against the distance from the diseased leaf for two different wind speeds: 0.5 m/s (*B*) and 1.5 m/s (*C*). All distances were measured horizontally (directly downwind) from the leaf on the extended cold-stage platform. Each box corresponding to a distance in the plots represents individual measurements from six separate papers across the three trials.

Fig. 3 *B* and *C* shows the results of the analysis from the synergistic wind and condensation experiments. Regardless of the wind velocities, spore-laden droplets were found mostly within 45 cm from the diseased leaf. For the higher wind speed of 1.5 m/s, a considerable number of droplets (≈ 80 across three trials) with or without spores traveled as far as 1.5 m, more than three times the maximum distance traveled by droplets in 0.5-m/s wind. Conversely, with higher wind speed, the total number of dispersed droplets (with or without spores) captured by the water-sensitive papers decreased significantly (≈ 640 for 0.5 m/s compared with ≈ 400 for 1.5-m/s wind speed across three trials). One possibility is that the higher wind speed reduces the number of jumping droplets by disrupting the diffusive flow field that was growing the droplets to promote coalescence. However, it is also possible the higher wind speed actually increases the number of dispersed jumping droplets, due to the decreased thickness of the laminar boundary layer over the leaf. If the latter effect outcompetes the former, the reduced number of captured droplets/spores at higher wind speeds can be rationalized by the fact that many of the droplets simply travel beyond the range of the water-sensitive papers. Wind speed measurements above the individual papers along the $\alpha = 0°$ line (*SI Appendix*, Fig. S13) for $V_{wind} = 1.5$ m/s revealed a wind speed of about 0.9 m/s over the farthest paper (≈ 140 cm from the leaf). This wind speed is significant enough to carry the spores farther, validating our intuition about the spatial limitation associated with this wind study.

A control experiment was also run, for a diseased leaf without any condensation, to compare the relative importance of wind-induced dry dispersal of spores. For capturing the dry spores, we replaced the water-sensitive papers with adhesive papers. For both the 0.5- and 1.5-m/s wind speeds, no spores were captured by any of the adhesive papers. This is consistent with previous reports on the removal of dry brown rust spores, which found that appreciable spore liberation occurs for wind speeds of at least 1.3 m/s when subjected to short bursts of increasing wind speeds (32) or 4 m/s for continuous wind (17). Theoretical calculation also suggests a critical wind speed value in the range of 2 to 10 m/s for the dry micrometric spore removal from the leaf surface (*SI Appendix*, section 5). It can therefore be concluded that jumping-droplet condensation is necessary for spores to get liberated under a moderate wind speed, with the wind solely assisting the subsequent dispersal.

Quantifying the Total Number of Dispersed Spores. While Fig. 3 quantifies the number of spores dispersed to a given location downwind, it cannot capture the total number of spores being carried away from the diseased leaf. To resolve the latter, we placed a single water-sensitive paper just downwind of the diseased leaf, with the paper held perpendicular to the leaf plane (Fig. 4*A*). As before, we performed three trials for both $V_{wind} = 0.5$ and 1.5 m/s, using leaves from the same diseased plant to minimize trial-to-trial variability.
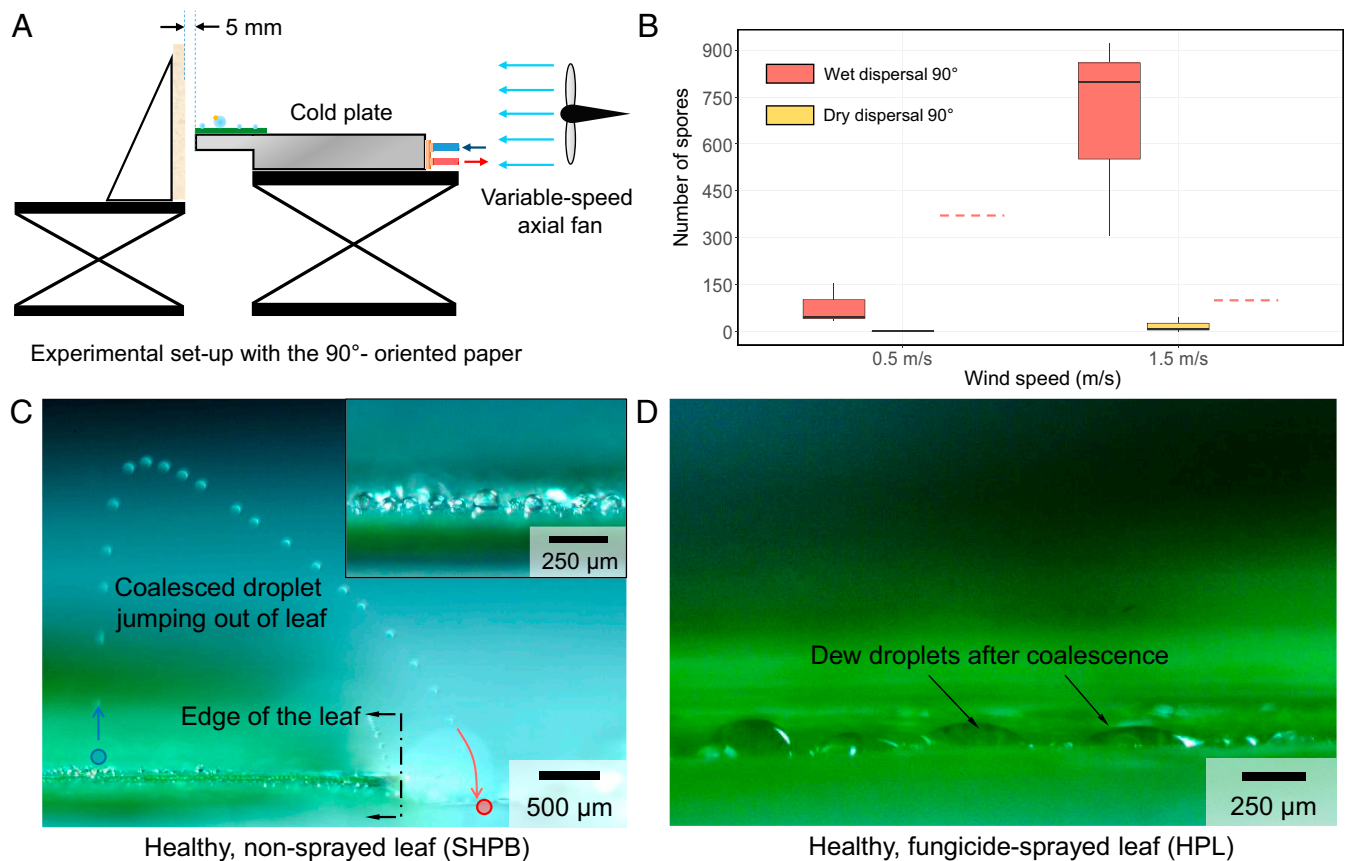
Fig. 4. Effectiveness of wet dispersal over dry dispersal of spores. (*A*) A modification of the spore-capturing setup was used to maximize spore capture in wet (both wind and condensation on leaf) and dry dispersal (only wind; no condensation on leaf). A water-sensitive paper or adhesive paper was placed perpendicular to the diseased leaf on the cold stage, depending on wet or dry dispersal. A variable-speed fan was placed upstream of the leaf to ensure spore dispersal from the leaf. (*B*) Plot comparing the number of spores captured with jumping-droplet condensation on diseased leaves in the presence of wind (wet dispersal; red) and spore dispersal via wind only without any condensation (dry dispersal; yellow). The dashed red lines for both wind speeds show the total number of captured spores in the long-distance setup of Fig. 3 *B* and *C*. (*C*) Chronophotograph of a jumping dew droplet on a healthy wheat leaf. Even with no applied wind (only the laboratory's natural air circulation), the jumped droplet could travel over the edge of the leaf. The blue circle shows the coalescence event that initiated the droplet jumping, while the red circle shows the final impact location beyond the leaf's edge. In *Inset*, a magnification of the quasispherical dew droplets is shown, indicating the superhydrophobic (SHPB) contact angle. (*D*) After a healthy leaf was sprayed with fungicide, the contact angle was dramatically decreased to render it hydrophilic (HPL). Coalescence of growing dew droplets now resulted in filmwise condensation, rather than jumping-droplet condensation.

The fan was turned on after enough condensate droplets appeared on the diseased leaf (≈ 30 min), and the water-sensitive paper was analyzed after each 1-h experiment (*SI Appendix*, Fig. S4B). As a control test, we also ran the experiment without any condensation on the diseased leaves (dry dispersal) and using a dry adhesive paper as the perpendicular surface.

The results plotted in Fig. 4B show a complete picture of the spore dispersal via condensation and wind. The median number of spores captured with $V_{\text{wind}} = 1.5$ m/s was about 800 compared with about 50 for $V_{\text{wind}} = 0.5$ m/s, an order of magnitude higher. This reveals that the higher wind speed is a net benefit to the number of dispersed droplets/spores (i.e., the benefit of a thinner boundary layer outcompetes the detriment of a reduced rate of condensation growth). In other words, going back to the setup in Fig. 3, these present findings indicate there were actually more jumped droplets traveling in the wind for $V_{\text{wind}} = 1.5$ m/s, despite the fact that more were able to settle downward for collection onto the papers for $V_{\text{wind}} = 0.5$ m/s. Of course, in actual crop fields, the magnitude of dew-induced spore dispersal will depend upon the supersaturation (i.e., rate of growth and coalescence events) and duration of a dew cycle.

The trend of the perpendicular paper capturing more spores at a higher wind speed was also observed for the case of dry dispersal. We found no spores on the adhesive paper for $V_{\text{wind}} = 0.5$ m/s and a maximum of 44 spores at $V_{\text{wind}} = 1.5$ m/s. This is consistent with a previous study on the wind removal of brown rust spores (*Puccinia recondita* f. sp. *tritici*, now known as *P. triticina*), which reported 1.3 m/s as the threshold wind velocity (32). However, perhaps the most significant aspect of the results presented in Fig. 4B is the stark contrast in the number of spores collected in dry dispersal (i.e., only wind) vs. a dew cycle where condensation and wind work together. For $V_{\text{wind}} = 1.5$ m/s, comparing values of the highest number of spores collected for the dry dispersal (44 for one trial) with the lowest number for a dew cycle (305 for one trial) shows that jumping dew droplets are the primary liberation mechanism for moderate winds, with the wind mostly serving to boost dispersal. The importance of the dew cycle is even more stark for $V_{\text{wind}} = 0.5$ m/s, as no spores could be collected from wind alone, but a minimum of 33 spores were found during a dew cycle. The results of Figs. 3 and 4 *A* and *B* show that even in the absence of any rain or strong wind (a necessary precondition for a moderate to heavy dew formation), fungal pathogens can still spread via jumping-droplet condensation on the wheat leaves.

Mukherjee et al.
Synergistic dispersal of plant pathogen spores by jumping-droplet condensation and wind

PNAS | 5 of 8
https://doi.org/10.1073/pnas.2106938118

For all experiments performed here, the leaves were always fixed to a horizontally oriented cold plate. This is hardly the case for natural wheat leaves, which can be oriented in all possible inclinations and bend/twist when subjected to wind flow (33). We suggest that this experimental limitation does not affect the key findings of this study, as it serves as a conservative estimate to spore dispersal. For the no-wind condition, an inclined leaf would likely increase the number of spore-laden droplets able to jump beyond the leaf's edge while additionally enabling gravitational rolling for larger droplets (34). Under windy conditions, the resulting oscillations would likely increase the number of coalescence events for enhanced droplet jumping (35) and gravitational shedding.

How does spore dispersal from jumping dew and wind compare with rain-induced dispersal? Pathogen dispersal due to raindrop impact occurs via both vortex-induced dry dispersal (11) and splashed droplets (12). A previous study experimentally demonstrated that a 4.9-mm-diameter raindrop impacting a wheat leaf liberated about 8,000 rust spores for a release height of 5 cm and 60,000 for a release height of 100 cm (36). Their corresponding simulation indicated that for a rain intensity of 10 $\mathrm{mmh^{-1}}$, about 2.5^{10} to 10^{10} total spores would be removed over a 5-min period. This number dwarfs the number of spores being liberated and dispersed from jumping dew and a gentle wind, which we measured as roughly 100 to 1,000 spores/h for each diseased leaf (refer to Fig. 4B). However, we argue that as dew cycles in nature regularly occur in the complete absence of rain, these two modes of spore dispersal are complementary rather than in direct competition.

Suppression of Jumping-Droplet Condensation on Wheat Leaves. Now that we have identified the synergistic roles of jumping-droplet condensation and wind flow for liberating and dispersing spores, we should consider potential disease mitigation strategies. One approach is to suppress the jumping-droplet effect, which would remove the liberation mechanism that necessarily precedes wind-assisted dispersal. Previous studies of jumping-droplet condensation on engineered surfaces have shown that a superhydrophobic nanostructure is necessary for inflating dew droplets to the quasispherical contact angles required for coalescence-induced jumping (19, 20, 37–39). Here, we apply a commonly used fungicide that is known to increase the leaf's wettability from superhydrophobic to hydrophilic (13). Given that the growth and jumping hydrodynamics of dew droplets are not appreciably influenced by the presence of fungal spores (17), for simplicity, we compared condensation on healthy leaves that were either sprayed or not sprayed with the fungicide. On a healthy, nonsprayed leaf, deposited water droplets exhibited advancing and receding contact angles of $\theta_A = 142.4° \pm 1.6°$ and $\theta_R = 138° \pm 2.6°$, respectively. This low–contact angle hysteresis ($\theta_A - \theta_R < 10°$) is indicative of the low-adhesion Cassie state (40), confirming the surface is effectively superhydrophobic. In contrast, when the healthy leaves are sprayed with a fungicide (*Materials and Methods*) and dried before condensation, the advancing contact angle ranges widely from $\theta_A = 0°–59°$, and the receding contact angle is almost 0.

Rather than using water-sensitive paper to indirectly characterize jumping behavior, we observed the condensing leaf directly using side-view high-speed microscopy. From Fig. 4C, *Inset*, it can be seen that the dew droplets retain the large (superhydrophobic) contact angles exhibited by deposited droplets. As expected from its superhydrophobic surface wettability, the growth and coalescence of micrometric dew resulted in the jumping-droplet effect for nonsprayed leaves (Fig. 4C). Even in the absence of any detectable wind, successive coalescence events resulted in jumped droplets depositing beyond the edge of the leaf. The hydrophilic sprayed leaves, on the other hand,

grew dew droplets with hydrophilic contact angles that culminated in filmwise condensation (Fig. 4D and Movie S2). These high-adhesion, low-angle droplets are inherently inimical to coalescence-induced jumping. Thus, we have shown that a simple application of a fungicide can suppress the condensation-induced liberation of spores from the leaf surface.

Rendering the wheat leaves hydrophilic might have some undesired side effects, as the wax coating on wheat leaves helps them conserve water in dry conditions (41). Moreover, rendering the leaves hydrophilic changes the dynamics of raindrops impacting the leaves. For example, Park et al. (13) observed that splashed droplets tended to rebound from unsprayed leaves but stick to leaves treated with fungicide. When splashed droplets contain spores, this increased surface adhesion might therefore enhance disease spread. Thus, although the application of a hydrophilic spray has the clear benefit of inhibiting spore transport via jumping-droplet condensation, future studies could explore whether this has the unintended consequence of enhancing spore transport by rain splash.

Given that a number of previous reports have shown jumping-droplet condensation on natural surfaces, including wheat leaves (17), lotus leaves (42), and cicada wings (43), proper contextualization of our current work is warranted. While our previous study demonstrated the jumping-droplet–induced liberation of fungal spores from wheat leaves (17), liberation alone is a necessary but not sufficient condition for any disease epidemic. In this study, we have extensively looked into the subsequent dispersal/deposition of the spores on a wide spatiotemporal scale, necessary to facilitate large-scale disease dissemination (44). We found that even without any detectable wind, rust spores can be liberated and transported to neighboring plants solely via jumping dew droplets. We also showed that long-range dispersal of spore-laden jumped droplets is possible at low windspeeds. Similar wind, on the other hand, is unable to liberate and disperse dry spores from the leaf surface. This strongly establishes the importance of the dew-induced spore liberation mechanism in wheat crops. A simple and cost-effective solution to suppress the jumping-droplet condensation on wheat leaves is also introduced in this study.

Conclusion
Jumping-droplet condensation has only recently been discovered as a fungal spore liberation mechanism for wheat leaves (17). Here, we have shown that even in the absence of any rain or significant wind, jumping-droplet condensation is sufficient to launch pathogenic matter away from a wheat leaf for local dispersal. Further, in the presence of a low wind flow, we have shown that jumped droplets can clear the boundary layer to enable long-range dispersal in the wind. Although our discussion was centered around wheat leaves, there is a wide variety of superhydrophobic plants (42, 45–47) where jumping droplet–induced pathogen liberation and dispersal could be similarly important. We were able to completely suppress the jumping-droplet effect by applying a common fungicide to increase the surface wettability of the wheat leaves. These findings indicate that the application of a hydrophilic spray could be a simple yet effective solution for halting the ability of dew cycles to spread disease across crops. Future research could determine whether the jumping-droplet effect could alternatively be halted by seeing how the leaf wettability varies with differing cultivar architectures.

Materials and Methods
Preparation of Wheat Leaves. A mixed seed of two winter wheat lines Massey and VA-135, both known to be susceptible to leaf rust, were provided by the Griffey Laboratory at Virginia Tech. The growth and inoculation processes of the plants are the same as those described in previous reports

(11, 17). The mature leaves were cut from the stem and used within 6 h for the experiments. After pustules of *P. triticina* spores broke through the leaf epidermis, the loose spores remained on the leaf surface as single spores or as clusters (*SI Appendix*, Fig. S2 C, D).

Experimental Setup. For all the condensation-induced and dry spore dispersal experiments, a section of a diseased wheat leaf was bonded with thermal grease (Thermalcote; 251G-ND) to a cold plate attached to a chilled recirculator (Fischer Scientific; 13874647). Each leaf section was ∼3-cm long and was taken from the middle portion of a wheat leaf, where the width was fairly uniform and ∼1 cm (*SI Appendix*, Fig. S1). The cold plate was custom machined, such that three of the leaf section's four edges perfectly aligned with the edges of the plate. Due to the varying laboratory ambient temperature and humidity, the cold plate temperatures were varied across the experiments while maintaining a supersaturation of $S = 1.5 \pm 0.3$. Jumped droplets from the leaf sections were captured on 76- × 26-mm water-sensitive papers (Syngenta; 347456). The condensation experiments were started only after the cold plate temperature reached the set value and significant condensate droplets appeared on the leaf surface. All experimental trials were run for 1 h. Three such 1-h trials were run for each scenario (no wind, $V_{wind} = 0.5$ m/s, $V_{wind} = 1.5$ m/s, and dry dispersal). Wind experiments were done using either of the two variable-speed fans (AC Infinity; Multifan S1 or TerraBloom; TB-MFIF-6). In all the experiments involving wind, to achieve the desired wind speed above the leaf, the speed of the fan and the distance between the fan and the leaf were changed. Wind speed measurements were done 1 cm above the leaf and the water-sensitive papers with an anemometer (Omega; model no. HHF81). For the no-wind experiments, the anemometer was used to confirm a zero wind speed in the laboratory. While there was some minor air circulation in the laboratory that sometimes boosted the lateral movement of jumping droplets, it was always beneath the anemometer's minimum measurable wind speed of 0.4 m/s. For the dry dispersal of spores with only wind and no condensation on the leaf, 3- × 5-inch adhesive papers (Sensor; Yellow Pest Monitoring Cards) were used to capture the dry spores from the leaf.

Image Analysis. The stain-patterned water-sensitive papers were collected at the end of a condensation experiment trial (*SI Appendix*, Fig. S4). The papers were then analyzed under an optical microscope (Nikon; model: Eclipse LV150) with a 10× objective lens (Mitutoyo; M Plan APO). Due to the magnified field of view being much smaller than the paper dimensions, we used a live image–stitching software (Microvisioneer; Manual Whole Slide Imaging) to obtain a composite image of all spores and droplet stains. The stitched images were then analyzed in Qupath, an open source image analysis software. For the dry dispersal experiments, the same technique was used to count the spores.

Fungicide Spraying on Healthy Leaves. A fungicide solution was prepared by mixing 80-ppm fungicide (Bayer CropScience; Proline 480 SC Fungicide) and 125-ppm surfactant (Winfield Solutions; TopSurf) in water. A previous report (13) has specific details on the fungicide and surfactant constituents. An atomizer (Portable SprayerSystem; Preval 267) was used to spray this solution on the healthy wheat leaf sections. For a uniform coating, the sprayer was held about 5 cm above a leaf section and sprayed while guiding it back and forth once, along the length of the leaf. Contact angle measurements and video imaging of coalescence on these sprayed leaves were done after the leaves were dried for at least 2 h under a fume hood.

Imaging. A high-speed color camera (Vision Research; Phantom v711) was used to capture the jumping-droplet liberation and drift from the healthy wheat leaves as well as the coalescence of condensing droplets on the fungicide-sprayed wheat leaves. All the videos were captured at 7,500 frames per second at 1,024 × 768 resolution.

Contact Angle Measurements. Advancing and receding contact angles of water droplets on healthy wheat leaves (both nonsprayed and fungicide sprayed) were measured with a goniometer (Ramé-Hart; Model 590). A 10-μL water droplet was deposited on the surface, and the shrink/swell method was used to find the advancing and receding contact angles.

Data Availability. All study data are included in the article and/or supporting information.

1. D. E. Aylor, The role of intermittent wind in the dispersal of fungal pathogens. *Annu. Rev. Phytopathol.* **28**, 73–92 (1990).
2. C. T. Ingold, *Spore Discharge in Land Plants* (Clarendon Press, Oxford, United Kingdom, 1939).
3. F. Liu et al., Asymmetric drop coalescence launches fungal ballistospores with directionality. *J. R. Soc. Interface* **14**, 20170083 (2017).
4. M. W. F. Fischer, J. L. Stolze-Rybczynski, Y. Cui, N. P. Money, How far and how fast can mushroom spores fly? Physical limits on ballistospore size and discharge distance in the Basidiomycota. *Fungal Biol.* **114**, 669–675 (2010).
5. L. Yafetto et al., The fastest flights in nature: High-speed spore discharge mechanisms among fungi. *PLoS One* **3**, e3237 (2008).
6. H. A. McCartney, Dispersal of spores and pollen from crops. *Grana* **33**, 76–80 (1994).
7. A. Bainbridge, B. J. Legg, Release of barleymildew conidia from shaken leaves. *Trans. Br. Mycol. Soc.* **66**, 495–498 (1976).
8. D. E. Aylor, Force required to detach conidia of *Helminthosporium maydis*. *Plant Physiol.* **55**, 99–101 (1975).
9. K. D. Srivastava, L. M. Joshi, S. Nagarajan, Liberation of uredospores of *Puccinia recondita tritici* under varying wind speeds. *Indian Phytopathol.* **40**, 474–477 (1987).
10. J. M. Hirst, O. J. Stedman, Dry liberation of fungus spores by raindrops. *J. Gen. Microbiol.* **33**, 335–344 (1963).
11. S. Kim, H. Park, H. A. Gruszewski, D. G. Schmale III, S. Jung, Vortex-induced dispersal of a plant pathogen by raindrop impact. *Proc. Natl. Acad. Sci. U.S.A.* **116**, 4917–4922 (2019).
12. T. Gilet, L. Bourouiba, Fluid fragmentation shapes rain-induced foliar disease transmission. *J. R. Soc. Interface* **12**, 20141092 (2015).
13. H. Park et al., Dynamics of splashed droplets impacting wheat leaves treated with a fungicide. *J. R. Soc. Interface* **17**, 20200337 (2020).
14. I. Sache, Short-distance dispersal of wheat rust spores. *Agronomie* **20**, 757–767 (2000).
15. B. D. L. Fitt, H. A. McCartney, P. J. Walklate, The role of rain in dispersal of pathogen inoculum. *Annu. Rev. Phytopathol.* **27**, 241–270 (1989).
16. S. Nagarajan, D. V. Singh, Long-distance dispersion of rust pathogens. *Annu. Rev. Phytopathol.* **28**, 139–153 (1990).
17. S. Nath et al., 'Sneezing' plants: Pathogen transport via jumping-droplet condensation. *J. R. Soc. Interface* **16**, 20190243 (2019).
18. J. B. Boreyko, C. H. Chen, Self-propelled dropwise condensate on superhydrophobic surfaces. *Phys. Rev. Lett.* **103**, 184501 (2009).
19. F. Liu, G. Ghigliotti, J. J. Feng, C. H. Chen, Numerical simulations of self-propelled jumping upon drop coalescence on non-wetting surfaces. *J. Fluid Mech.* **752**, 39–65 (2014).
20. R. Enright et al., How coalescing droplets jump. *ACS Nano* **8**, 10352–10362 (2014).
21. C. L. Campbell, L. V. Madden, *Introduction to Plant Disease Epidemiology* (John Wiley & Sons, 1990).
22. D. Aylor, A framework for examining inter-regional aerial transport of fungal spores. *Agric. For. Meteorol.* **38**, 263–288 (1986).
23. J. K. M. Brown, M. S. Hovmøller, Aerial dispersal of pathogens on the global and continental scales and its impact on plant disease. *Science* **297**, 537–541 (2002).
24. H. A. McCartney, B. D. L. Fitt, "Dispersal of foliar fungal plant pathogens: Gradients and spatial patterns" in *The Epidemiology of Plant Diseases*, D. B. Jones, Ed. (Springer, 1998), pp. 138–160.
25. M. Abichou, B. de Solan, B. Andrieu, Architectural response of wheat cultivars to row spacing reveals altered perception of plant density. *Front. Plant Sci* **10**, 999 (2019).
26. X. Qu et al., Self-propelled sweeping removal of dropwise condensate. *Appl. Phys. Lett.* **106**, 221601 (2015).
27. X. Chen, J. A. Weibel, S. V. Garimella, Exploiting microscale roughness on hierarchical superhydrophobic copper surfaces for enhanced dropwise condensation. *Adv. Mater. Interfaces* **2**, 1400480 (2015).
28. X. Yan et al., Droplet jumping: Effects of droplet size, surface structure, pinning, and liquid properties. *ACS Nano* **13**, 1309–1323 (2019).
29. H. Lamb, *Hydrodynamics* (Dover Publications, New York, 1945).
30. R. C. Faulwetter, Wind-blown rain, a factor in disease dissemination. *J. Agric. Res.* **10**, 639–648 (1917).
31. D. Beysens et al., Application of passive radiative cooling for dew condensation. *Energy* **31**, 2303–2315 (2006).
32. L. Geagea, L. Huber, I. Sache, Removal of urediniospores of brown (*Puccinia recondita* f.sp. *tritici*) and yellow (*P. striiformis*) rusts of wheat from infected leaves submitted to a mechanical stress. *Eur. J. Plant Pathol.* **103**, 785–793 (1997).
33. S. Gart, J. E. Mates, C. M. Megaridis, S. Jung, Droplet impacting a cantilever: A leaf-raindrop system. *Phys. Rev. Appl.* **3**, 044019 (2015).
34. R. Mukherjee, A. S. Berrier, K. R. Murphy, J. R. Vieitez, J. B. Boreyko, How surface orientation affects jumping-droplet condensation. *Joule* **3**, 1360–1376 (2019).
35. C. H. Chen et al., Dropwise condensation on superhydrophobic surfaces with two-tier roughness. *Appl. Phys. Lett.* **90**, 173108 (2007).

Mukherjee et al.
Synergistic dispersal of plant pathogen spores by jumping-droplet condensation and wind

PNAS | 7 of 8
https://doi.org/10.1073/pnas.2106938118

36. L. Geagea, L. Huber, I. Sache, Dry-dispersal and rain-splash of brown (*Puccinia recondita* f.sp. tritici) and yellow (*P. striiformis*) rust spores from infected wheat leaves exposed to simulated raindrops. *Plant Pathol.* **48**, 472–482 (1999).

37. R. Enright, N. Miljkovic, A. Al-Obeidi, C. V. Thompson, E. N. Wang, Condensation on superhydrophobic surfaces: The role of local energy barriers and structure length scale. *Langmuir* **28**, 14424–14432 (2012).

38. T. Mouterde *et al.*, Antifogging abilities of model nanotextures. *Nat. Mater.* **16**, 658–663 (2017).

39. M. D. Mulroe, B. R. Srijanto, S. F. Ahmadi, C. P. Collier, J. B. Boreyko, Tuning superhydrophobic nanostructures to enhance jumping-droplet condensation. *ACS Nano* **11**, 8499–8510 (2017).

40. D. Quéré, Non-sticking drops. *Rep. Prog. Phys.* **68**, 2495–2532 (2005).

41. X. Liu *et al.*, Experimental study of leaf wax n-*alkane* response in winter wheat cultivars to drought conditions. *Org. Geochem.* **113**, 210–223 (2017).

42. G. S. Watson, M. Gellender, J. A. Watson, Self-propulsion of dew drops on lotus leaves: A potential mechanism for self cleaning. *Biofouling* **30**, 427–434 (2014).

43. K. M. Wisdom *et al.*, Self-cleaning of superhydrophobic surfaces by self-propelled jumping condensate. *Proc. Natl. Acad. Sci. U.S.A.* **110**, 7992–7997 (2013).

44. B. D. L. Fitt, P. H. Gregory, A. D. Todd, H. A. McCartney, O. C. Macdonald, Spore dispersal and plant disease gradients: A comparison between two empirical models. *J. Phytopathol.* **118**, 227–242 (1987).

45. B. Mockenhaupt, H. J. Ensikat, M. Spaeth, W. Barthlott, Superhydrophobicity of biological and technical surfaces under moisture condensation: Stability in relation to surface structure. *Langmuir* **24**, 13591–13597 (2008).

46. C. Neinhuis, W. Barthlott, Characterization and distribution of water-repellent, self-cleaning plant surfaces. *Ann. Bot. (Lond.)* **79**, 667–677 (1997).

47. K. Koch, W. Barthlott, Superhydrophobic and superhydrophilic plant surfaces: An inspiration for biomimetic materials. *Philos. Trans.- Royal Soc., Math. Phys. Eng. Sci.* **367**, 1487–1509 (2009).